ELSEVIER

International Journal of Coal Geology 49 (2002) 33–55

International Journal of COAL GEOLOGY

www.elsevier.com/locate/ijcoalgeo

The Donets Basin (Ukraine/Russia): coalification and thermal history

R.F. Sachsenhofer [a,*], V.A. Privalov [b], M.V. Zhykalyak [c], C. Bueker [d,1], E.A. Panova [e], T. Rainer [a], V.A. Shymanovskyy [a,f], R. Stephenson [g]

[a] *Institut für Geowissenschaften, Montanuniversität Leoben, Peter-Tunner-Strasse 5, A-8700 Leoben, Austria*
[b] *Donetsk State Technical University, Artem str., UA-84000 Donetsk, Ukraine*
[c] *Donetsk State Regional Geological Survey, Sybirtseva str. 17, UA-84500 Artemovsk, Ukraine*
[d] *Institute of Geology, and Geochemistry of Petroleum and Coal, Aachen University of Technology, Lochnerstr. 4-20, D-52056, Germany*
[e] *UkrNIMI, Tchelyuskintsev str. 291, UA-83121 Donetsk, Ukraine*
[f] *Technological Centre of Ukrgeofisika, S. Perofska str. 10, UA-03057 Kyiv, Ukraine*
[g] *Research School of Sedimentary Geology, Vrije Universiteit, De Boelelaan 1085, 1081 HV Amsterdam, Netherlands*

Received 27 April 2001; accepted 19 October 2001

Abstract

The Donets Basin (Donbas) is one of the major late Paleozoic coal basins in the world. The Donbas Foldbelt is an inverted part of the Donets Basin characterized by WNW–ESE-trending folds and faults. The age of basin inversion is under discussion. Large parts of the Donets Basin host anthracite and meta-anthracite. Low-rank coals are restricted to the western and northern basin margins. Vitrinite reflectance patterns along the Gorlovka Anticline indicate syn-deformational coalification. Vitrinite reflectance isolines are displaced along thrusts, clear evidence that main coalification predates late faulting. 1-D and 2-D numerical models were applied to elucidate the factors that control coalification in the western Donets Basin (Krasnoarmeisk Monocline, Kalmius–Torets Depression, South Syncline). The models indicate that the depth of the seams and the heat flow during maximum (Permian) burial are the most important parameters. The thickness of late Carboniferous and Permian rocks increased from the southwestern basin margin towards the basin center. Permian erosion along the Krasnoarmeisk Monocline and in the Kalmius–Torets Depression was on the order of 2–3 km. More rocks were eroded southeast of the Donetsk–Kadievka Fault Zone (4–5 km). Heat flow during maximum burial was in the range of 40–75 mW/m^2. Heat flow in the Krasnoarmeisk Monocline and the Kalmius–Torets Depression increased in a northeastward direction from 40 to 55 mW/m^2. Heat flow at the eastern edge of the Kalmius–Torets Depression and in the South Syncline was in the range of 60–75 mW/m^2 and increased towards the southeast. The resulting coalification pattern in this area was overprinted by thermal events in the northern Krasnoarmeisk Monocline and the South Syncline. These are probably related to (Permian?) magmatic intrusions. Coked coal occurs at the contact to presumed Permian sills and dikes southwest of Donetsk.

Keywords: Coalification; Donetsk; Ukraine; Thermal history; Magmatism; Numeric modelling

1. Introduction

The Donets Basin (Donbas) occupies the southeastern part of the Dniepr–Donets Basin. It covers an area

* Corresponding author. Tel.: +43-3842-402-788; fax: +43-3842-402-9902.
E-mail address: sachsenh@unileoben.ac.at (R.F. Sachsenhofer).
[1] Present address: NAM, Assen, Netherlands.

0166-5162/02/$ - see front matter
PII: S0166-5162(01)00063-5

of 60,000 km^2 and contains one of the major coal fields in the world. The basin lies mainly in the Ukraine with the eastern part of the coal field extending into Russia. The basin fill contains Devonian pre- and syn-rift rocks and a complete Carboniferous post-rift sequence several thousand metres thick. A major part of the Donets Basin has been inverted and is named Donbas Foldbelt (Fig. 1).

Although major progress has been achieved in the understanding of Donets Basin, there also remain numerous questions (cf. Stephenson et al., 2001). These include (i) the mechanisms resulting in the excessively thick post-rift Carboniferous succession compared to the degree of tectonic activity recorded in the basin architecture; (ii) the precise timing and the tectonic events leading to profound Permian uplift and erosion; and (iii) the timing of the formation of large linear folds, reverse faults and thrusts in the Donbas Foldbelt.

The Carboniferous sequence contains about 130 workable coal seams. Seam thickness varies between 0.45 and 2.5 m and averages 0.9 m. The Donbas coals usually have high ash yields (12–18%) and high sulphur contents (2.5–3.5%, Panov, 1999). The average methane content of coal is 14.7 m^3/t (Marshall et al., 1996). Coal rank in the Donets Basin is generally high and reaches the meta-anthracite stage. Low-rank coals are restricted to the western and northern basin margins. Commercial reserves in the Ukrainian part were estimated during Soviet times to be 23,700 Mt of coal. However, according to Walker (2000), they appear overestimated under current economic conditions.

In the present paper, we apply basin modelling techniques to reconstruct the factors that control coalification patterns in the Donets Basin. Apart from coalification, the knowledge of the thermal history is interesting for different aspects of the evolution of the Donets Basin, including the heat flow distribution during maximum Permian burial, the estimation of the thickness of eroded rocks and the timing of coal bed methane generation. The reconstructed thermal histories also contribute to a better understanding of the origin of epigenetic mineral deposits in the Donets Basin, including mercury, antimony, lead, zinc, and gold. These deposits are probably related to post-Carboniferous magmatic activity (Nikolskiy et al., 1973; de Boorder et al., 1996; Aleksandrov et al., 1996).

2. Geological setting

2.1. Basin structure

The Donets Basin is the southeastern segment of the Dniepr–Donets Basin, a Late Devonian rift structure located on the southern part of the Eastern European craton (Stovba and Stephenson, 1999; Fig. 1). The boundary between the Donets and Dniepr segments is defined as the Mariupol–Kursk Lineament (de Boorder et al., 1996; see insert in Fig. 1). The Moho beneath the Donets Basin is at 40 km depth (DOBREfraction Working Group, 2001), whereas it is at about 35–40 km depth beneath the Dniepr segment. The Dniepr–Donets Basin continues westward into the relatively shallow Pripyat Trough, and eastward into the Karpinsky Swell. The basement is formed by crystalline rocks of the Eastern European craton. These are overlain with an erosional unconformity by middle Devonian to Carboniferous rocks, which reach a thickness of more than 20 km thick (Chekunov et al., 1993).

The structure of the Donbas Foldbelt, which is the inverted part of the Dniepr–Donets Basin, is dominated by WNW–ESE-striking anticlines and synclines. The Gorlovka (Main) Anticline is the largest fold. It is almost symmetric with steeply dipping limbs (60°–80°, Fig. 3). The anticline is bounded by the North and South Synclines (Fig. 1). Major thrusts occur along the northern margin of the basin. Minor folds, reversed faults and rotated fault blocks occur along the southern boundary of the basin. The age of the compressional structures is a matter of controversy. Following traditional ideas, Privalov et al. (1998) assume a dominantly Permian (Hercynian) age, whereas Stovba and Stephenson (1999) favour a dominantly late Cretaceous (Alpine) age.

The southwestern part of the Donets Basin comprises the Krasnoarmeisk Monocline and the Kalmius–Torets Depression. The NE-ward-dipping rocks of the Krasnoarmeisk Monocline overlie the Mariupol–Kursk Lineament. Towards the east, the Krasnoarmeisk area grades into the Kalmius–Torets Depression, which represents the intersection of the northwestern continuation of the SE-trending South Syncline with the SW-trending Voltchansk synform. The eastern margin of the Kalmius–Torets Depression is located near Donetsk and Makeevka. It is formed by a set of NE-trending faults, which may be the surface expres-

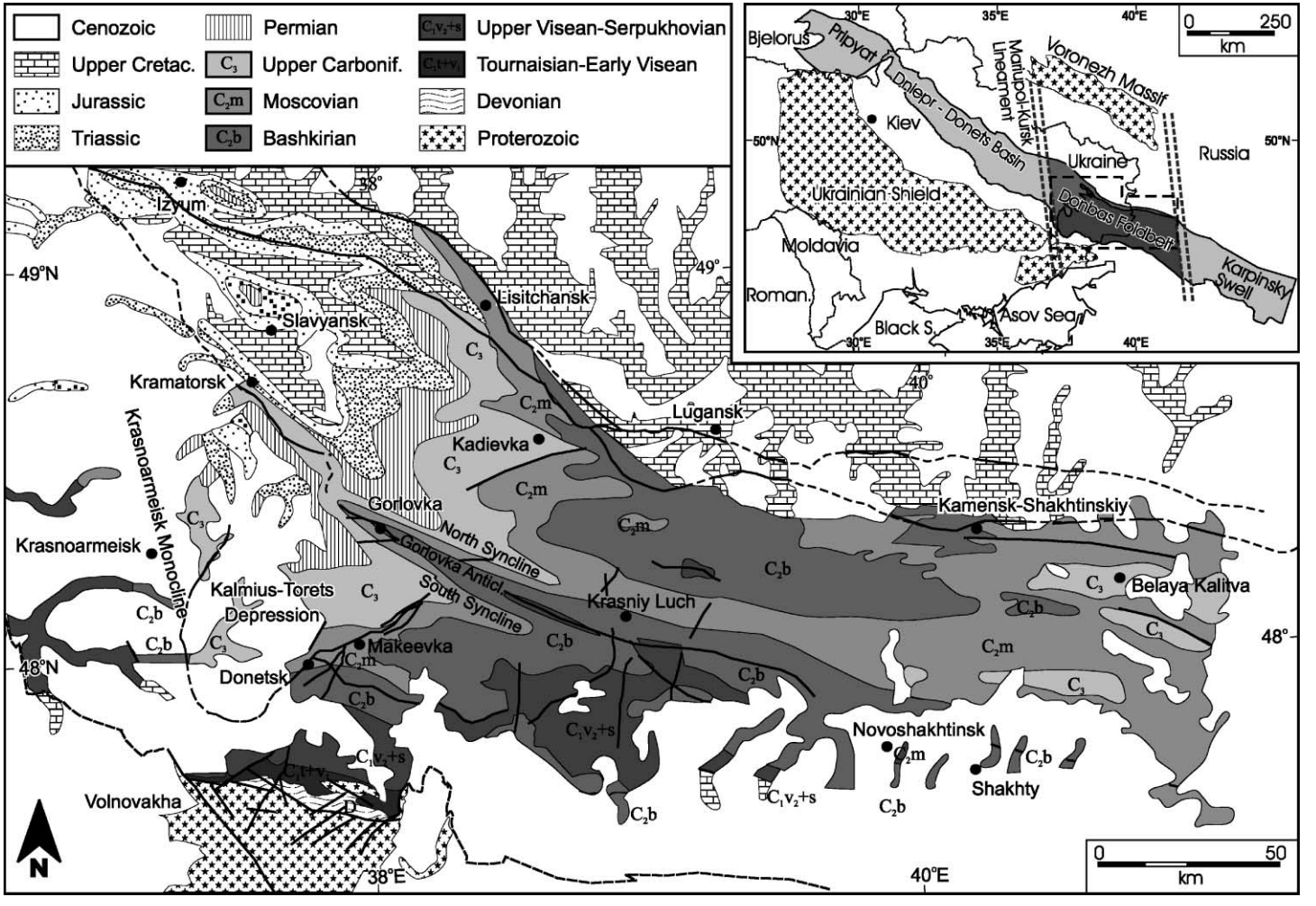

Fig. 1. Location of the study area and geologic sketch map of the Donets Basin (modified after Minesterstvo Geologii SSSR, 1983).

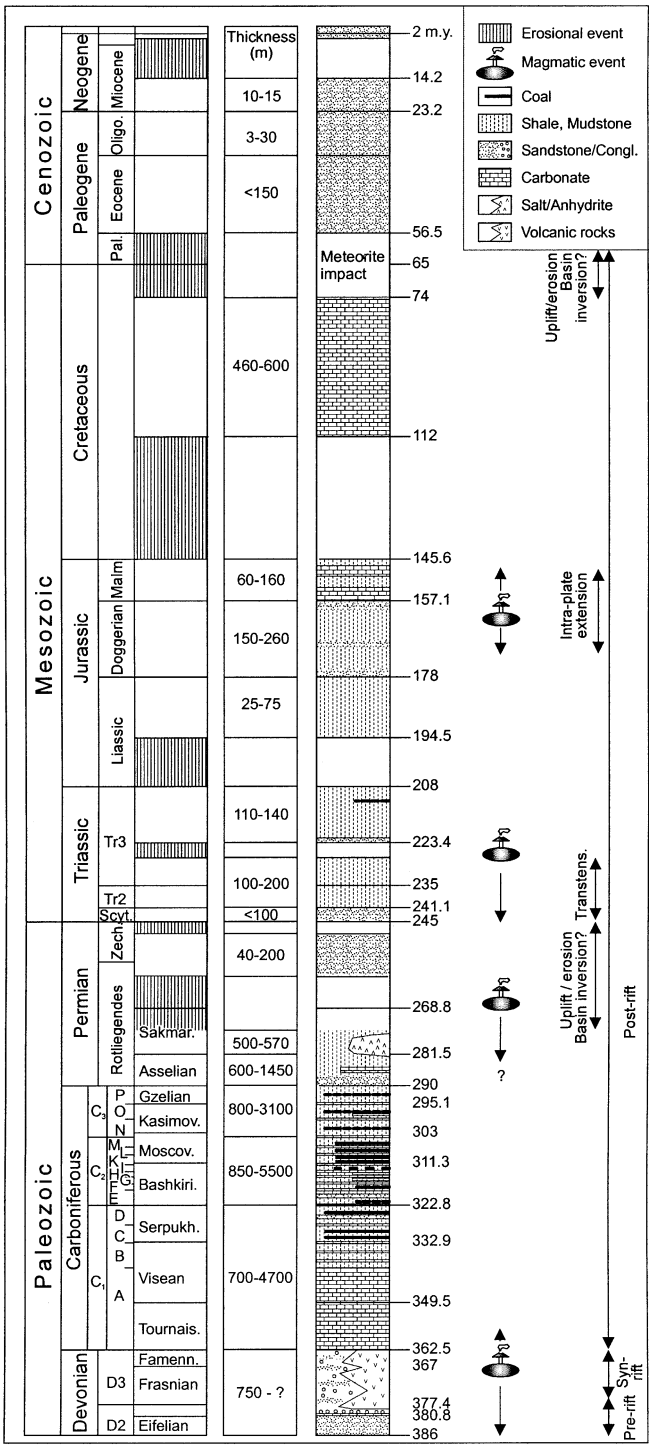

Fig. 2. Chrono- and lithostratigraphy of the Donets Basin. Major magmatic and tectonic events are also shown (Sterlin et al., 1963; Belokon, 1971; Einor, 1996; Privalov et al., 1998; Stovba and Stephenson, 1999). Time-scale after Harland (1990).

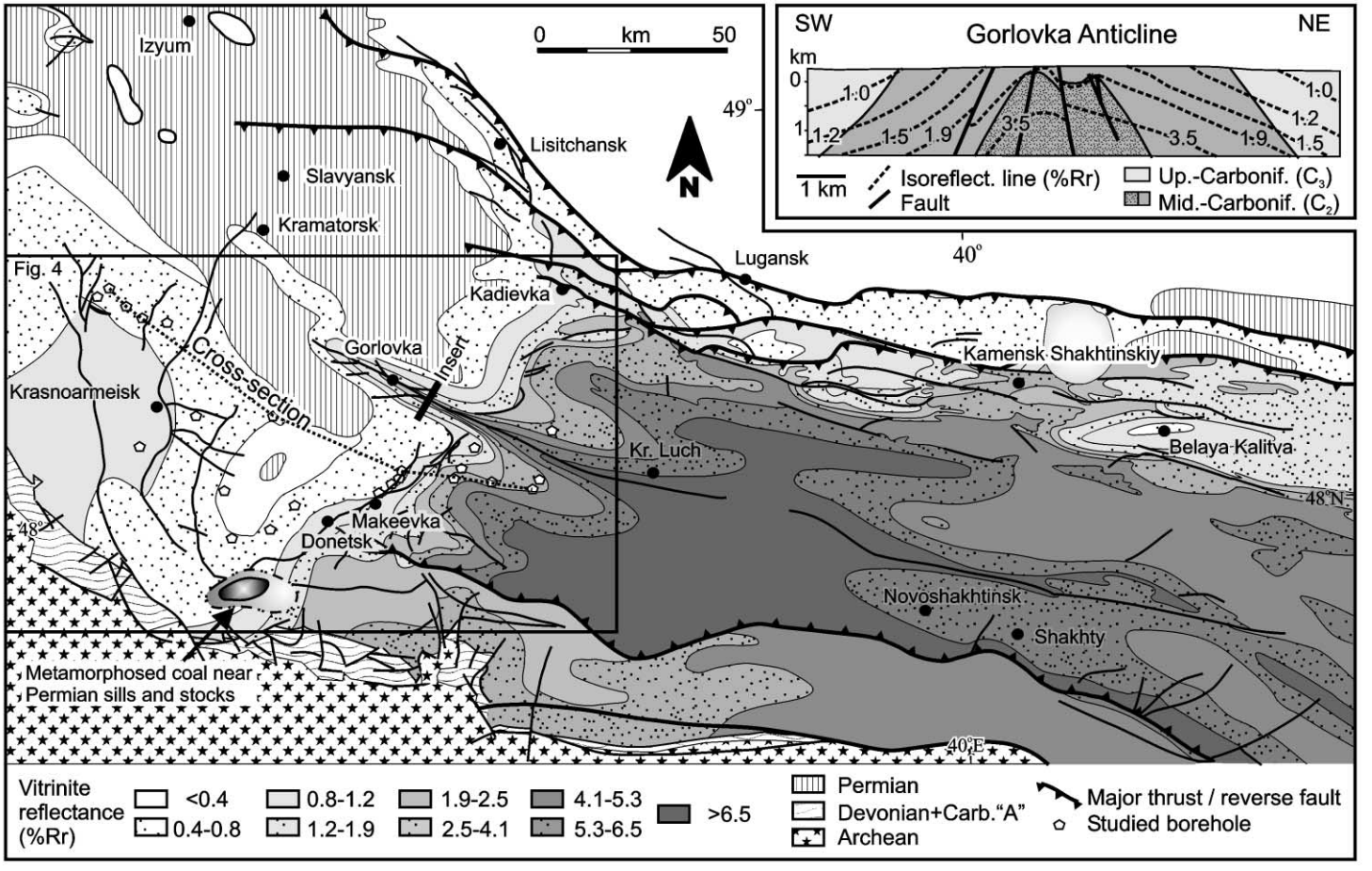

Fig. 3. Coalification map at the top of the Carboniferous sequence (modified after Levenshtein et al., 1991b). The insert shows a cross section through the Gorlovka Anticline.

sion of a deep basement fault (Donetsk–Kadievka Fault Zone; Fig. 4).

2.2. Basin evolution

2.2.1. Devonian syn-rift phase

Main rifting occurred during Late Devonian time. van Wees et al. (1996) reconstructed stretching factors up to 1.3 for the northwestern Dniepr–Donets Basin, but emphasize that conventional lithospheric stretching and thermal subsidence models fail in the southeastern part. The total thickness of Devonian pre- and syn-rift rocks exposed along the southern margin of the Donets Basin is 750 m, including thick volcanic rocks (Fig. 2). The thickness of Devonian rocks along the basin center is unknown, but may reach 5 km.

2.2.2. Late Paleozoic post-rift phase

Major post-rift subsidence occurred during the Permo-Carboniferous. The Carboniferous sequence is subdivided into lower (C_1), middle (C_2), and upper Carboniferous (C_3) rocks. These are further subdivided into lithostratigraphic units named suites (Makarov, 1982, 1985). C_1 is composed from bottom to top of suites A–D, C_2 comprises suites E–M, and C_3 contains suites N–P. Their correlation with the standard time-scale is presented in Fig. 2 (see also Izart et al., 1996). Suites C, K, L and M are especially rich in coal (Levenshtein et al., 1991a). However, coal seams and intercalations of coal are present throughout the Carboniferous succession. Permian rocks are preserved along the western and northern margins of the Donets Basin, where they are represented by a sand–shale series with sparse interbeds of coals and limestone (Nesterenko, 1978). Thick evaporites occur in Asselian and Sakmarian levels. Whereas extensive syn-rift magmatism occurred in most of the Dniepr–Donets Basin, post-rift magmatic rocks have been described only in the Donets Basin. They include Carboniferous (ultra-)basic stocks and dikes, and Permian

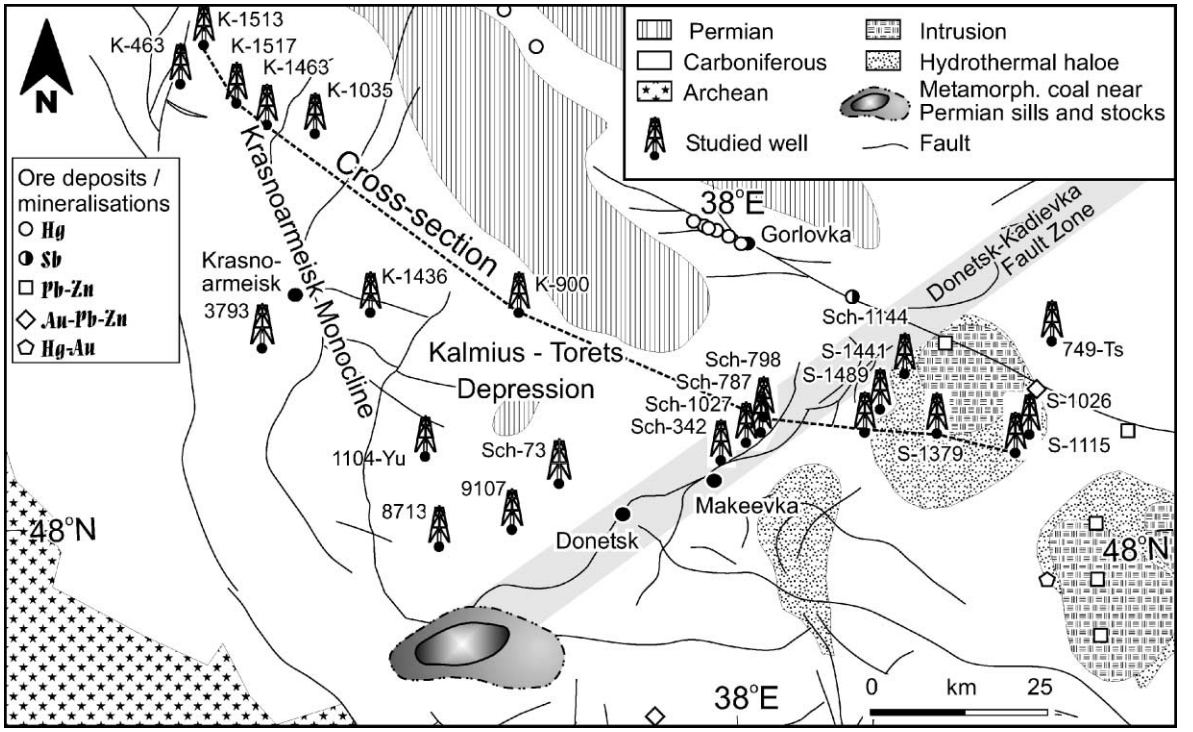

Fig. 4. Position of the modelled wells and the cross section in the western Donets Basin (see Fig. 3 for location of map). The position of intrusive bodies and respective hydrothermal haloes (Aleksandrov et al., 1996) is indicated together with the location of epigenetic mineral deposits and occurrences (Lazarenko et al., 1975).

(~ 290–260 m.y.) trachyliparites (e.g. Lazarenko et al., 1975; Stovba and Stephenson, 1999; Fig. 2). The presence of early Permian salt tectonics in the Donets Basin is controversial. However, a preliminary interpretation of deep seismic reflection data suggests that there may be Devonian salt at depth coring the Gorlovka Anticline (DOBREflection Working Group, 2000).

2.2.3. Permian uplift

Within the Donbas Foldbelt, Permian rocks and significant parts of the Carboniferous sequence were eroded during a major Permian uplift phase. Its mechanisms are still poorly understood and may be related to the build-up of stresses emanating from the Hercynian Caucasus/Uralian orogens or to the activity of an asthenospheric diapir (cf. Stephenson et al., 2001). Using coalification data, Nagorny and Nagorny (1976) estimated Permian erosion to be as much as 11 km along the central part of the basin and up to more than 15 km along its southern margin. Stovba and Stephenson (1999) suggest erosion of up to 10 km based on extrapolations of missing stratigraphy in view of seismic evidence. Many authors assume that basin inversion occurred during Permian uplift (e.g. Privalov, 1998).

2.2.4. Mesozoic–Cenozoic post-rift phase

Only relatively thin rocks, separated by unconformities, were apparently deposited during the Mesozoic and Cenozoic (Fig. 2). Magmatic events occurred during (trans-)tensional stages and produced Triassic (~ 230–200 m.y.) (trachy-)andesites and Jurassic (~ 160 m.y.) lamprophyres (e.g. Lazarenko et al., 1975; de Boorder et al., 1996; Privalov, 2000; Fig. 2). Using magnetic data, deep seismic sounding data and field observations, Aleksandrov et al. (1996) mapped large hidden intrusions and their hydrothermal haloes in the western Donets Basin. The authors advocate for a Late Permian (Triassic?) age of the intrusion and discuss a relation to epigenetic ore deposits in the Donets Basin (Nikolskiy et al., 1973; de Boorder et al., 1996). The locations of the postulated intrusive bodies and some ore deposits are shown in Fig. 4.

A minor uplift phase occurred during late Cretaceous to early Tertiary time. According to Stovba and Stephenson (1999), this was the time of major compression and basin inversion. In the latest Cretaceous time, a meteorite impact formed a large crater east of Kamensk–Shaktinsky (Grieve, 1982; Movshovich and Milyavsky, 1985).

2.3. Coalification

Coalification patterns in the Donets Basin were mapped by Levenshtein et al. (1991b; Fig. 3). Iso-

Table 1
Lithological composition of Carboniferous suites in different regions of the Donets Basin (after Levenshtein et al., 1991a)

Suite	Sandstone (%)	Siltstone (%)	Mudstone (%)	Limestone (%)	Coal (%)
All regions					
P	47.0	28.0	24.0	1.0	
O	32.0	40.0	25.0	3.0	
Krasnoarmeisk Monocline + Central Kalmius–Torets Depression					
N	18.6	37.0	43.0	1.2	0.2
M	37.0	34.0	26.0	2.2	0.8
L	33.0	36.0	25.0	3.1	2.9
K	45.0	27.0	25.0	2.3	0.7
I	34.0	25.0	39.0	1.7	0.3
H	27.0	39.0	32.0	1.8	0.2
G	16.0	45.0	37.0	1.5	0.4
F	26.0	35.0	35.0	3.6	0.4
Eastern Kalmius–Torets Depression					
N	27.4	33.0	38.5	0.8	0.4
M	29.0	66.7		3.1	1.2
L	41.0	54.0		2.5	2.5
K	36.2	61.0		1.6	1.2
I	33.0	65.0		1.5	0.5
H	28.0	70.5		0.5	1.0
G	20.0	79.0		0.6	0.05
F	23.7	72.0		4.0	0.3
South Syncline/North Syncline					
N	32.2	32.5	33.6	1.3	0.4
M	24.0	51.5	20.7	3.0	0.8
L	41.0	36.0	18.8	2.4	1.8
K	36.0	44.5	15.7	3.0	0.8
I	30.9	41.0	27.0	0.7	0.4
H	33.0	47.9	17.7	0.7	0.7
G	32.3	30.4	36.6	0.5	0.2
F	39.0	39.7	20.3	0.92	0.08
All regions					
E	14.0	48.0	32.0	6.0	
D	25.0	45.0	28.0	2.0	
C	16.0	53.0	29.0	2.0	
B	19.0	58.0	20.0	3.0	
A				100.0	

Table 2
Physical properties assigned to standard lithotypes used for simulations

Lithotype	Density [kg/m^3]	Initial porosity	Compression [Pa^{-1}]		Matrix thermal conductivity [W/m K]		Heat capacity [cal/g K]		Permeability[a] at porosity of	
			Maximum	Minimum	0 °C	100 °C	20 °C	100 °C	5%	75%
Water	1160	0	2	1	0.60	0.68	0.999	1.008	1.0	1.0
Sandstone	2660	42	500	10	3.12	2.64	0.178	0.209	−2.0	0.0
Siltstone	2672	56	8000	10	2.14	2.03	0.201	0.242	−5.0	0.0
Mudstone	2680	65	60,000	10	1.98	1.91	0.213	0.258	−5.5	−1.0
Limestone	2710	42	300	25	2.83	2.56	0.195	0.223	−4.0	13.0
Coal	2000	52	130,000	10	0.50	0.46	0.204	0.248	−5.5	−1.0
Basement	2750	5	2	1	2.72	2.35	0.188	0.223	−16.0	−16.0

[a] Permeabilities (−5 means 10^{-5} md) are calculated for different stages of porosity.

reflectance lines generally follow the main structural elements, like antiforms and synforms. Breaks in coalification are observed across thrust planes. Coalification, therefore, is older than the main thrusting event. On the other hand, transects across the Gorlovka Anticline show that the dip of iso-reflectivity lines is gentle, whereas the dip of bedding planes is steep (Fig. 3). This is clear evidence that coalification along the Gorlovka Anticline predates the late stages of its formation, but postdates its early stages. Perhaps, the latter are related to (Early Permian?) salt tectonics.

The rank of specific stratigraphic units increases towards the basin center. For example, vitrinite reflectance of a coal seam in suite K (k_5) is below 0.6% R_r SW of Donetsk and N of Lugansk, but above 6.0% R_r near Krasnij Luch, despite a similar present-day elevation (sea level). In the literature (e.g. Nagorny and Nagorny, 1976), this is interpreted exclusively in terms of an increase of original upper Carboniferous and Permian overburden. Anomalously high coalification including natural coke is observed in close vicinity (several metres) to magmatic sills and stocks SW of Donetsk (e.g. Jernovaya, 1997; Fig. 3).

3. Methodology

3.1. Vitrinite reflectance

Random vitrinite reflectance (%R_r) of 131 coal samples was measured in the Leoben lab using a Leitz microscope and standard procedures (e.g. Taylor et al., 1998). The standard deviation was generally low (< 10% of the mean value). Information on vitrinite reflectance of 117 additional coal samples was taken from unpublished reports (Donetsk State Regional Geological Survey, Artemovsk). All vitrinite reflectance values were measured on coals and are therefore reliable, even if they were measured in different labs (Bostick and Foster, 1975). R_r values of well Sch-1144 was calculated using maximum (R_{max}) and minimum vitrinite reflectance (R_{min}) data and the equation $R_r = (R_{max} + R_{min})/2$. Most vitrinite

Fig. 5. (A) Subsidence and heat flow histories of well K-900. On the right, measured (dots) and calculated (lines) calibration data are shown. Shown isotherms are calculated using a heat flow of 56 mW/m^2, which results in a good fit between measured and calculated calibration data. Note that heat flow is only well defined for the time of maximum burial and for the present. (B) Calibration for an alternative model assuming that no information on lithologies would be available. Accepting a uniform sand–shale lithology, a good fit with vitrinite reflectance data would be achieved with a constant heat flow of 62 mW/m^2. (C) Calibration for models with modified subsidence histories. A good fit is obtained with a Permian heat flow of 60 mW/m^2 (erosion of a 1640-m-thick rock interval) and 53 mW/m^2 (erosion of a 2460-m-thick rock interval). (D) Models with modified Permo-Triassic heat flows. Heat flow peaks of 90 and 100 mW/m^2 result in a poor fit, whereas a heat flow peak of 110 mW/m^2 results in an unacceptable fit.

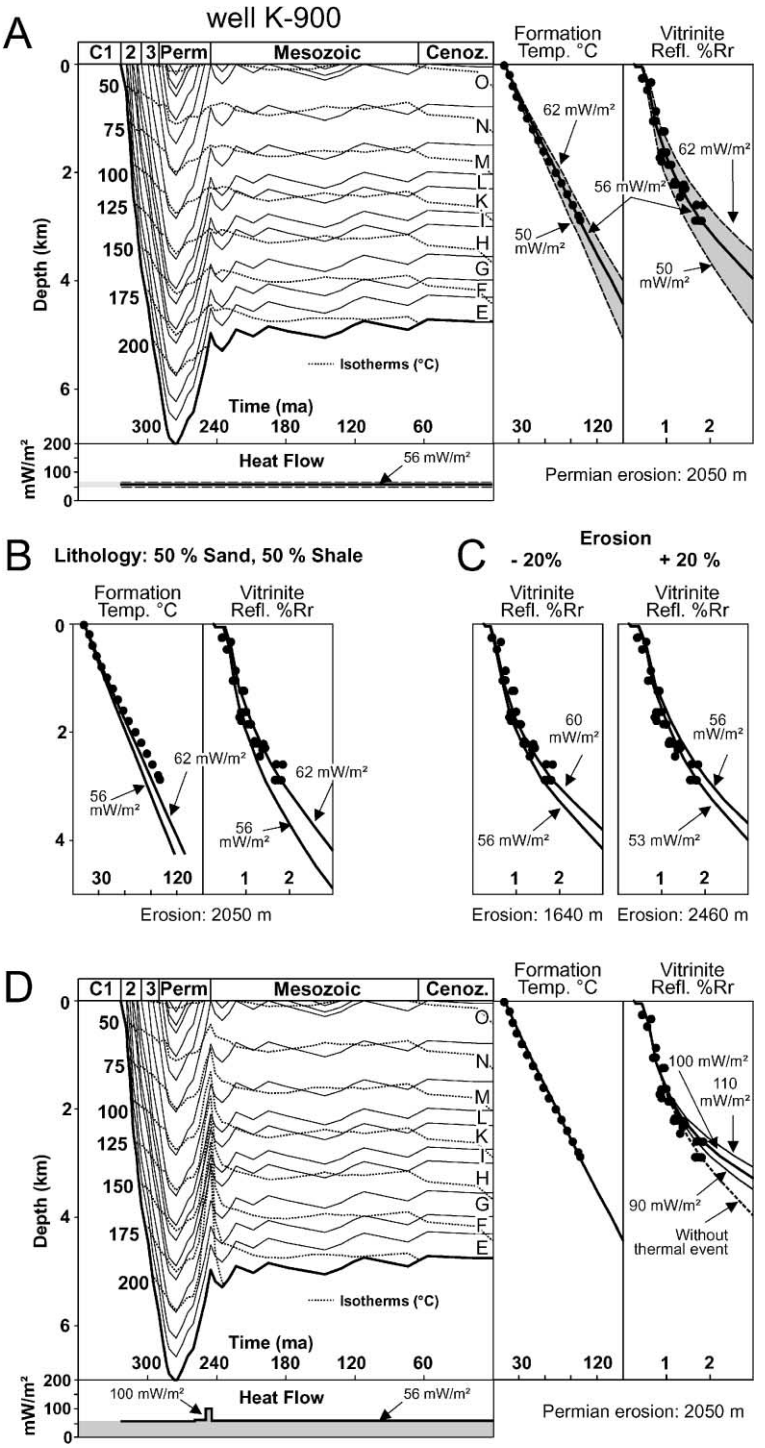
A
well K-900
C1
2
3
Perm
Mesozoic
Cenoz.
O
N
M
L
K
I
H
G
F
E
Depth (km)
Isotherms (°C)
Time (ma)
300
240
180
120
60
Heat Flow
56 mW/m²
mW/m²
Formation Temp. °C
Vitrinite Refl. %Rr
62 mW/m²
56 mW/m²
50 mW/m²
Permian erosion: 2050 m
B
Lithology: 50 % Sand, 50 % Shale
Erosion: 2050 m
C
Erosion
- 20%
+ 20 %
60 mW/m²
53 mW/m²
Erosion: 1640 m
Erosion: 2460 m
D
100 mW/m²
110 mW/m²
90 mW/m²
Without thermal event

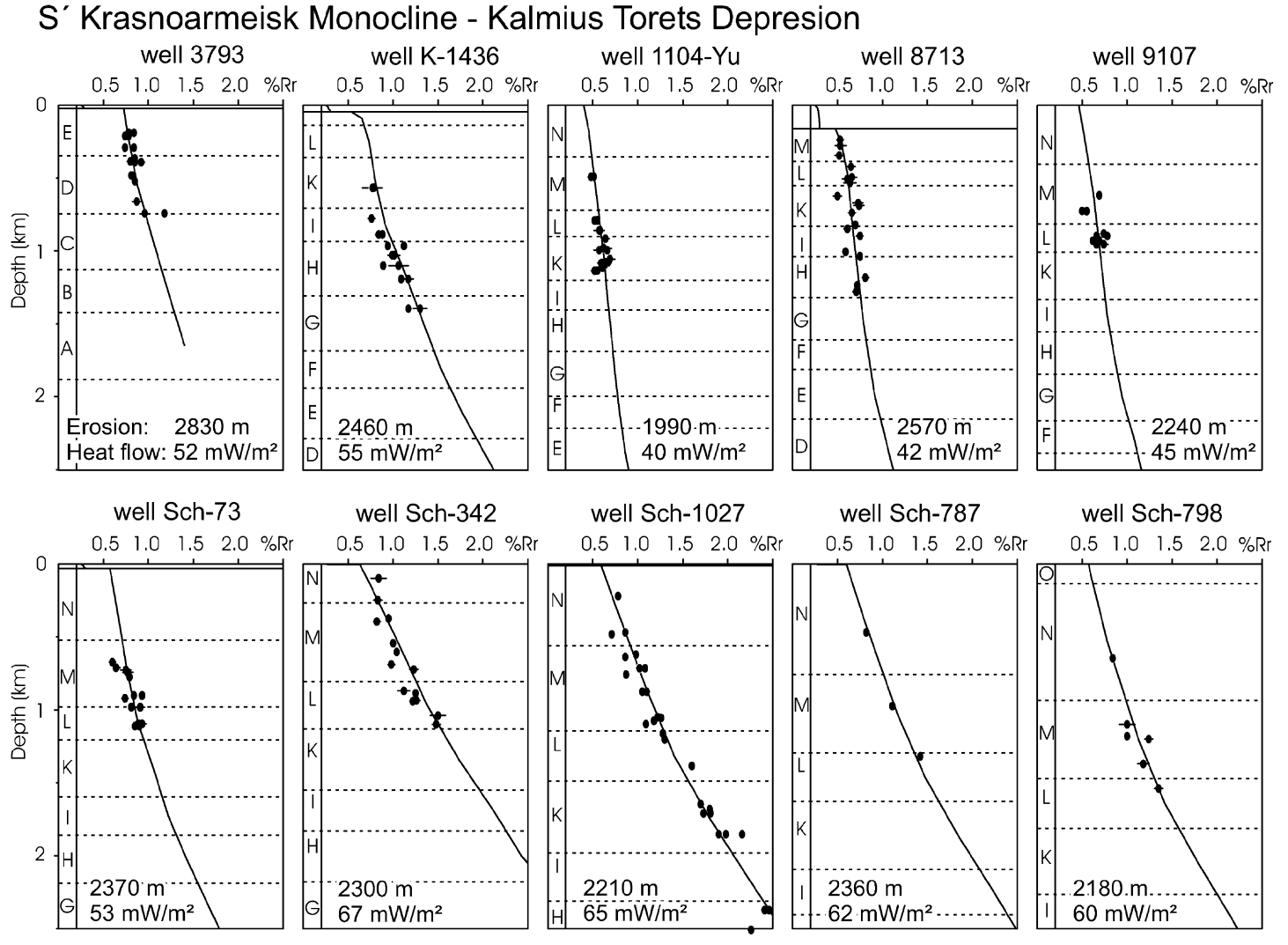

Fig. 6. Measured and calculated vitrinite reflectance (%R_r) for 10 wells in the southern Krasnoarmeisk Monocline and the Kalmius–Torets Depression. Values given in the boxes indicate the modelled Permian heat flow and the amount of eroded Paleozoic rocks. Capital letters represent Carboniferous suites (A–D: lower Carboniferous; E–M: middle Carboniferous; N–O: upper Carboniferous). See Fig. 4 for location of wells.

reflectance data are from middle and upper Carboniferous rocks. Data for lower Carboniferous rocks are available only for well 3793.

3.2. Thermal modelling

For thermal modelling, wells were selected, where vitrinite reflectance is below 6.0% R_r and where calibration data cover a depth interval of at least 750 m. These restrictions consider the applicability of algorithms for the calculation of vitrinite reflectance (see below) and the fact that the quality of heat flow reconstructions increases with the depth range of calibration data. Twenty-three wells, all located in the western Donets Basin, fulfilled these prerequisites (Fig. 4). For these wells and a NW–SE-trending cross section, paleo-heat flow was estimated using the basin modelling approach (Welte et al., 1997; Yalcin et al., 1997). Temperature modelling was performed with the PDI-1D™ and PetroMod 6.0 software packages of IES, Jülich. Calibration of the burial and heat flow histories was performed using R_r values and recent formation temperatures.

Input data for numeric models include the thickness of stratigraphic units, lithologies, rock physical parameters (e.g. thermal conductivities), the temperature at the sediment–water interface, and heat flow at the base of the Carboniferous sequence. Devonian syn-rift rocks are not considered. Detailed information on the thickness of the drilled suites and lithologic composition (percentages of sandstone, siltstone, mudstone/shale, coal, and limestone) for most wells was provided by the Donetsk State Regional Geological Survey. Average lithologic composition of specific suites in the Krasnoarmeisk, Kalmius–Torets, and South Syncline regions (Table 1) was used for suites which were not drilled in the respective well and for the 2-D model. The physical properties of standard lithologies which were used for the calculation of the mixed lithologies are shown in Table 2. See Büker (1996) and Hertle and Littke (2000) for a more detailed description of the calculation of physical properties of stratified bodies.

The above information was used to construct decompacted subsidence histories and the temperature field through time. The models were calibrated by modifying heat flow and the thickness of eroded rocks until a satisfactory fit between measured and calculated vitrinite reflectance and formation temperatures was obtained. We tried to keep heat flow histories as simple as possible. Therefore, we started with time-constant heat flows. If necessary, different heat flows for late Paleozoic and Mesozoic/Cenozoic times were adopted. In some wells, additional thermal events had to be included to obtain a good calibration. Heat flow variations associated with Devonian rifting are not considered in our models. This is because heat flow was elevated during Devonian rifting (up to 110 mW/m^2 according to models by Starostenko et al., 1999), but decreased rapidly during the post-rift stage. Middle and late Carboniferous heat flow (40–70 m.y. after rifting), therefore, was close to equilibrium (<60 mW/m^2; Starostenko et al., 1999).

In general, vitrinite reflectance is calculated using the kinetic EASY %R_o algorithm (Sweeney and Burnham, 1990). However, as this algorithm handles reflectances only up to 4.69% R_r, we used an extended version, which is calibrated to a maturity of 6.23% R_r (Everlien, 1996). Note, that up to 4.6% R_r, the models yield identical results.

4. Results

4.1. 1-D thermal models

4.1.1. Kalmius–Torets Depression, southern Krasnoarmeisk Monocline

Well K-900 is located NW of Donetsk. Models for this well are discussed in some detail to illustrate the basin modelling approach and to show some limitations. The subsidence history of well K-900 assuming Permian erosion of 2050-m-thick rocks is shown in Fig. 5. A heat flow of 56 mW/m^2 results in an excellent calibration (Fig. 5A) and is accepted as the most likely heat flow estimate.

Alternative models were introduced to check the sensitivity of the results. First, we used lower (50 mW/m^2) and higher heat flows (62 mW/m^2) which resulted in a poor fit (Fig. 5A). Second, the physical properties of the rocks were modified. For the original model, lithologies were created which consider detailed lithological information. For the alternative model, all lithologies were replaced by "shale + sandstone", simulating the case where no information on drilled lithotypes would be available. Because these lithologies

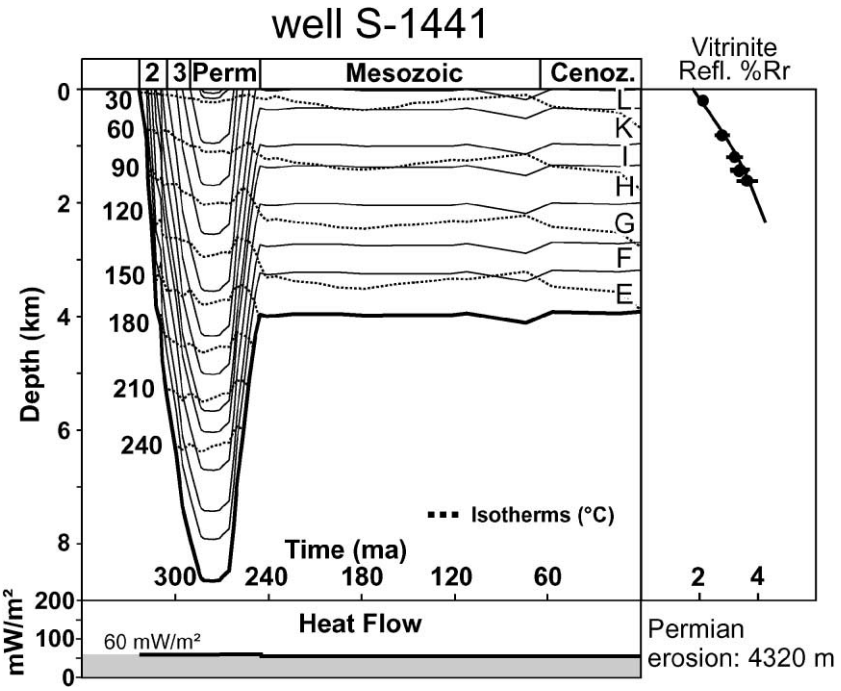

Fig. 7. Subsidence and heat flow histories of well S-1441. On the right, measured (dots) and calculated (lines) vitrinite reflectance data are shown. Note that heat flow is only well defined for the time of maximum burial.

are characterized by higher thermal conductivities than the coal-bearing lithotypes, the heat flow had to be increased to 62 mW/m^2 (Fig. 5B). Note that this scenario results in a poor fit with formation temperatures. Third, we modified the thickness of eroded Permo-Carboniferous rocks to 1640 and 2460 m and had to change heat flow to 60 and 53 mW/m^2, respectively (Fig. 5C). Thus, the alternative models suggest that the uncertainty of heat flow estimates in deep wells with good calibration data is only about 10%. The uncertainty concerning the thickness of eroded rocks is significantly higher.

Because vitrinite reflectance is mainly controlled by maximum temperatures, the above paleo-heat flow estimates are strictly valid only for the time of maximum burial (Permian). Carboniferous and Mesozoic heat flows cannot be determined precisely. However, it is possible to define an upper limit of possible heat flow ranges. Calculated vitrinite reflectance trends assuming Permo-Triassic heat flow events with 90, 100 and 110 mW/m^2 are shown in Fig. 5D. The first two models result in moderate to poor calibration, whereas the third model (110 mW/m^2) results in an unacceptable fit. Thus, Permo-Triassic heat flow definitely was not higher than 100 mW/m^2.

Thermal histories of 10 additional wells in the southern Krasnoarmeisk and Kalmius–Torets regions

Fig. 8. Subsidence and heat flow histories of well S-1379. On the right, measured (dots) and calculated (lines) calibration data are shown. (A) Adopting a simple thermal history (e.g. Permian heat flow of 65 mW/m^2; see also calculated isotherms) and Permian erosion of a 4740-m-thick Permo-Carboniferous rock interval results in poor calibration. The fit with vitrinite reflectance data cannot be improved by changing Permian heat flow to 55 or 75 mW/m^2 (dashed lines). (B) A good calibration is obtained with a high Paleozoic heat flow of 115 mW/m^2 and Permian erosion of a 2130-m-thick Permo-Carboniferous rock interval. Significantly more rocks have been eroded in neighbouring wells (e.g. S-1441; Fig. 7). Therefore, this model is not very likely. (C) A good calibration is also obtained with a subsidence history as in (A), a heat flow of 60 mW/m^2 during maximum burial, and a post-maximum burial heat flow event (180 mW/m^2). Note that the timing of the heat flow event is not well constrained.

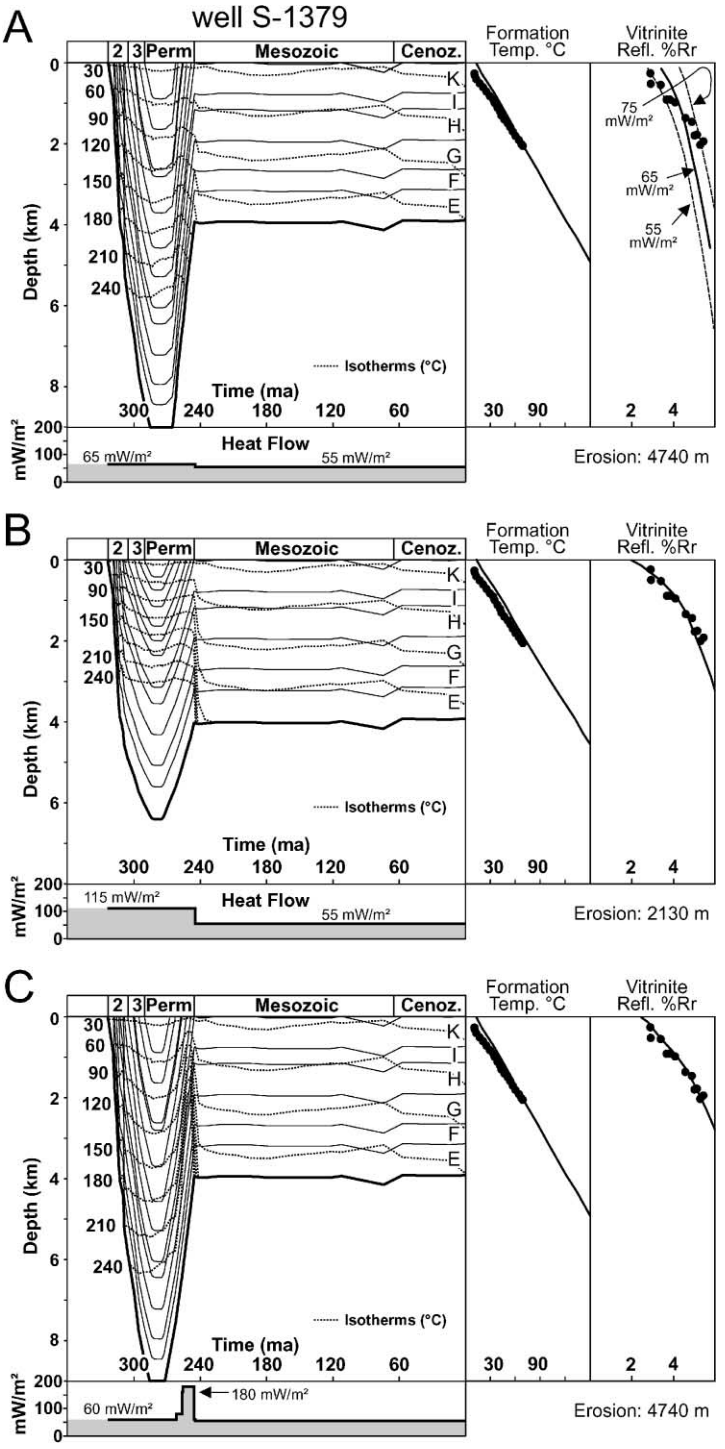
A
well S-1379
2
3
Perm
Mesozoic
Cenoz.
Formation Temp. °C
Vitrinite Refl. %Rr
K
I
H
G
F
E
75 mW/m²
65 mW/m²
55 mW/m²
Depth (km)
Isotherms (°C)
Time (ma)
Heat Flow
mW/m²
65 mW/m²
55 mW/m²
Erosion: 4740 m
B
115 mW/m²
Erosion: 2130 m
C
60 mW/m²
180 mW/m²
Erosion: 4740 m

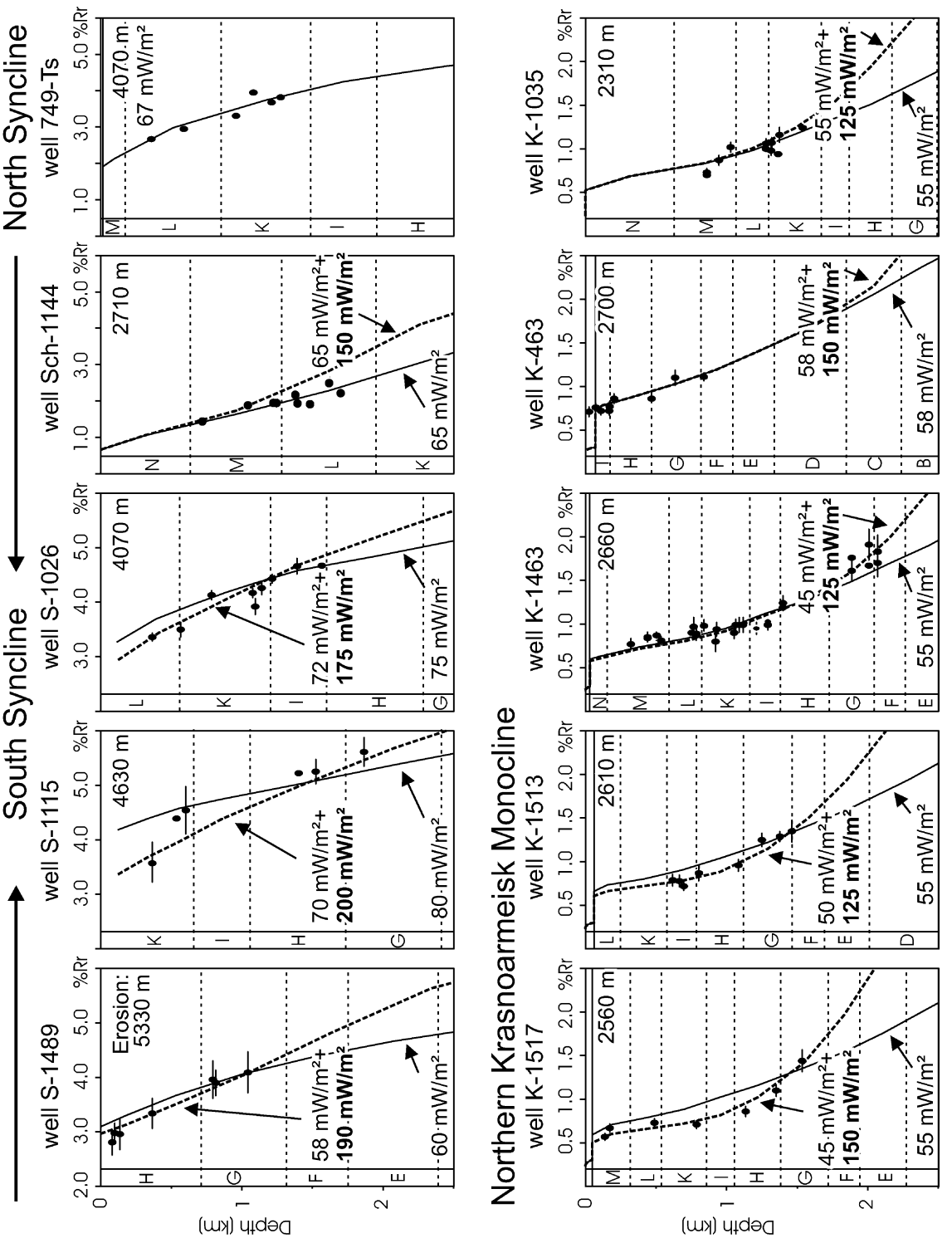
South Syncline
North Syncline
Northern Krasnoarmeisk Monocline
well S-1489
well S-1115
well S-1026
well Sch-1144
well 749-Ts
well K-1517
well K-1513
well K-1463
well K-463
well K-1035
Erosion: 5330 m
4630 m
4070 m
2710 m
4070 m
67 mW/m²
2560 m
2610 m
2660 m
2700 m
2310 m
58 mW/m²+ 190 mW/m²
70 mW/m²+ 200 mW/m²
72 mW/m²+ 175 mW/m²
65 mW/m²+ 150 mW/m²
45 mW/m²+ 150 mW/m²
50 mW/m²+ 125 mW/m²
45 mW/m²+ 125 mW/m²
58 mW/m²+ 150 mW/m²
55 mW/m²+ 125 mW/m²
60 mW/m²
80 mW/m²
75 mW/m²
65 mW/m²
55 mW/m²
55 mW/m²
55 mW/m²
58 mW/m²
55 mW/m²
Depth (km)
%Rr

were calibrated in similar ways. The thickness of Permo-Carboniferous rocks, which were eroded during the Permian and the applied heat flow values during maximum burial are presented together with calculated and measured calibration data in Fig. 6.

4.1.2. South Syncline, North Syncline

The South and North Synclines located southeast of Gorlovka are characterized by high-rank coals. Wells S-1441 and S-1379 are key wells for this area. In well S-1441, a good calibration is achieved applying a moderate heat flow during maximum burial (60 mW/m^2), and assuming that Permian erosion removed more than 4.3 km of rocks (Fig. 7). Although erosion cut into deeper stratigraphical levels (suite L) than in neighbouring wells in the Kalmius–Torets Depression (N, O), the result agrees with an observed eastward increase in the thickness of Permo-Carboniferous rocks (cf. Nagorny and Nagorny, 1976).

Erosion removed parts of suite K in well S-1379. Therefore, even more rocks should have been eroded in this well. In our model, we assume erosion of a 4740-m-thick rock interval. However, no fit between measured and calculated calibration data can be achieved using this estimate and a simple thermal history. Irrespective of using Permian heat flows of 55, 60, or 65 mW/m^2, the resulting vitrinite reflectance gradients are too low (Fig. 8A).

There are two ways to obtain a better calibration:

1. decreasing the thickness of eroded rocks to 2130 m and increasing heat flow during maximum burial to 115 mW/m^2 (Fig. 8B), or
2. introducing a high heat flow event, either before or after maximum burial. A scenario with a Permo-Triassic heat flow event is shown in Fig. 8C.

Scenario 1 is unlikely, because it implies a sharp eastward decrease in the original thickness of middle Carboniferous to lower Permian rocks. This is in contradiction with the general distribution of Paleozoic rocks in the Donets Basin (e.g. Maidanovitch and Radzivill, 1984). It also disagrees with an observed eastward increase in thickness of the preserved middle Carboniferous rocks. Thus, scenario 2 is accepted as more reasonable. The timing of the heat flow event is poorly constrained. However, some observations help to confine the age. Coalification patterns along the Gorlovka Anticline indicate syn-deformational coalification (Fig. 3) suggesting that heating occurred after the (post-Carboniferous) onset of deformation, but before the final stage. The age of final deformation along the Gorlovka Anticline is not yet solved finally. Most authors assume a Permian age (e.g. Zhykalyak et al., 2000); some authors favour a Cretaceous age (e.g. Stovba and Stephenson, 1999). Thus, at the moment, the heating event can be limited only to the time interval between the Permian and late Cretaceous. Several models differing in the timing of the heat flow event were established. The best calibration is obtained in models where the heat flow event occurs when erosion of Permo-Carboniferous rocks was advanced, but not yet completed (Fig. 8C). This suggests a late Permian age (248–257 m.y.) of heating, which was accepted in our 1-D models. However, as Permian uplift paths and Mesozoic subsidence curves are also not well constrained, later ages cannot be excluded.

Results from wells S-1489, S-1115, and S-1026 are not as clear. In these wells, a fair calibration is obtained applying simple heat flow histories with moderately high heat flows during maximum burial (60–80 mW/m^2). A better calibration is obtained using slightly lower heat flows during maximum burial (58–70 mW/m^2) and very high heat flows (175–200 mW/m^2) during a post-maximum burial heating event (Fig. 9). Calibration data in wells Sch-1144 and 746-Ts (North Syncline) are modelled using slightly elevated heat flows (65–70 mW/m^2) during maximum burial. Provided that post-maximum burial heat

Fig. 9. Measured and calculated vitrinite reflectance (%R_r) for wells in the South and North Synclines and in the northern Krasnoarmeisk region. For most wells, two heat flow scenarios were modelled. Models with a time-constant Permian heat flow (solid line) are indicated by a single heat flow value. Scenarios with an additional Permo-Triassic heating event (dotted line) are shown with two different heat flow values. The lower value refers to heat flow during maximum burial, the higher value (bold numbers) refers to the heating event. Values given in the upper right corner of the boxes indicate the amount of eroded Paleozoic rocks. Note that in wells S-1489, S-1115, S-1026, K-1517, K-1513, and K-1463, an additional heating event produces a better fit. Capital letters represent Carboniferous suites (A–D: lower Carboniferous; E–M: middle Carboniferous; N: upper Carboniferous). See Fig. 4 for location of wells and text for further explanations.

flow was elevated, it was definitely below 150 mW/m^2 (see Fig. 9).

4.1.3. Northern Krasnoarmeisk Monocline

Borehole K-1517 helps to unravel the thermal history of the northern Krasnoarmeisk Monocline (Fig. 9). In this well, a heat flow of 55 mW/m^2 and erosion of 2.5-km-thick rocks result in a poor calibration. A reduction of heat flow to 45 mW/m^2 during maximum burial and the introduction of a heat flow maximum of 150 mW/m^2, either before or after maximum burial, results in a significantly better fit. Similar heat flow histories result in a good calibration also in wells K-1513 and K-1463. This supports the presence of the additional heat flow maximum, although a simple heat flow history cannot yet be ruled out. Similar to the South Syncline, the age of the heating event cannot be determined exactly. A pre-maximum burial event cannot be excluded. If the heating event occurred after maximum burial, a slightly younger age (245–250 m.y.) than in the South Syncline corresponding to more advanced erosion has to be assumed.

In wells K-463 and K-1035, a good calibration is obtained without an "additional" heat flow event. However, as vitrinite reflectance in these cases is not sensitive to post-maximum burial heat flows up to 150 and 125 mW/m^2, respectively (Fig. 9), a heat flow event cannot be excluded.

4.1.4. Summary of 1-D models

Some major results of our 1-D models, which are important for 2-D modelling, are summarized in this section. The most important results are also displayed in Fig. 10. A more detailed evaluation follows in Section 5.

Heat flow during maximum burial was in the range of 40–75 mW/m^2 (Fig. 10A). Lateral heat flow variations are obvious. Along the modelled cross section (see below), Permian heat flow increased eastward.

There are convincing indications for a heating event occurring after maximum burial (late Permian?) in the South Syncline southeast of Gorlovka. This area coincides with one of the intrusions postulated by Aleksandrov et al. (1996; Fig. 10A). Therefore, we assume that magmatism was the main heat source. The applied 1-D software cannot handle magmatic intrusions. So, in the 1-D models, we increased heat flow (up to 200 mW/m^2) at the lower boundary of the model (base of Carboniferous).

1-D models suggest that the area north of Krasnoarmeisk also was exposed to a thermal event with heat flows up to 150 mW/m^2. In analogy to the eastern anomaly, we postulate a post-maximum burial event, which is slightly younger (245–250 m.y.) than the heating event in the South Syncline region (248–257 m.y.). Although no indications for a magmatic intrusion are known from this part of the basin, we speculate that magmatism occurred not only in the South Syncline region, but also in the Krasnoarmeisk region.

4.2. 2-D thermal model

4.2.1. General

The aim of the 2-D model is to test whether the thermal effects of magmatic intrusions are able to explain the observed coalification trends in the Krasnoarmeisk and South Syncline regions. For this, we modelled a 138-km-long WNW–ESE-trending transect connecting the thermal anomalies in the Krasnoarmeisk and South Syncline regions (Fig. 11A).

The computer-generated finite element model used for 2-D simulations is shown in Fig. 11B. The lower model boundary is defined by the base of the Carboniferous sequence. A total of 64 events and 203 grid-

Fig. 10. Results from 1-D models. (A) Heat flow distribution: The upper number indicates Permian heat flow during maximum burial. Two numbers separated by a slash refer to different thermal models (see Fig. 9). Note, that the left number is considered more reliable and was used to draw the shown hand-contoured isolines. The models suggest an additional heating event for the area southeast of Gorlovka (South Syncline) and the northern Krasnoarmeisk region (grey shading). Heat flow values during this thermal event are given by bold numbers. A magmatic heat source is suggested by the position of magmatic intrusions for the South Syncline (see Aleksandrov et al., 1996). (B) Map showing thickness of middle/upper Carboniferous (suite G to suite P) and lower Permian rocks. Hand-contoured isolines indicate a dramatic northeastward increase in thickness from the basin margin to the basin center. The thickness of rocks removed during Permian erosion is also indicated (negative numbers). Note a general eastward increase in erosion. Maximum values occur along antiforms, minimum values in synforms.

points was used to define the geological evolution. The calibration of the thermal history is based on eight wells.

Magmatic intrusions were introduced in the eastern and western sectors of the transects. Depth and lateral continuity of the intrusions were chosen to obtain a fit

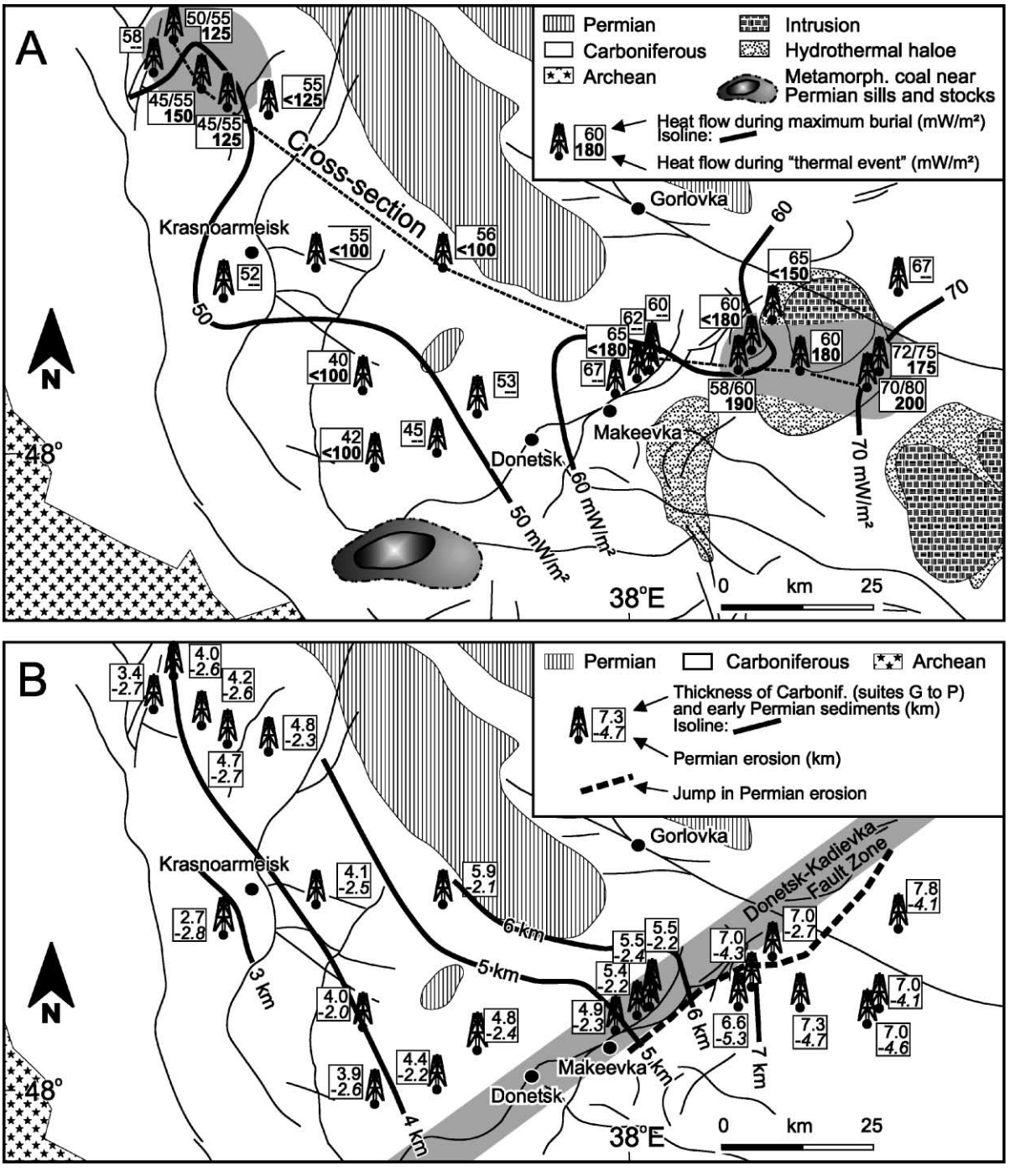

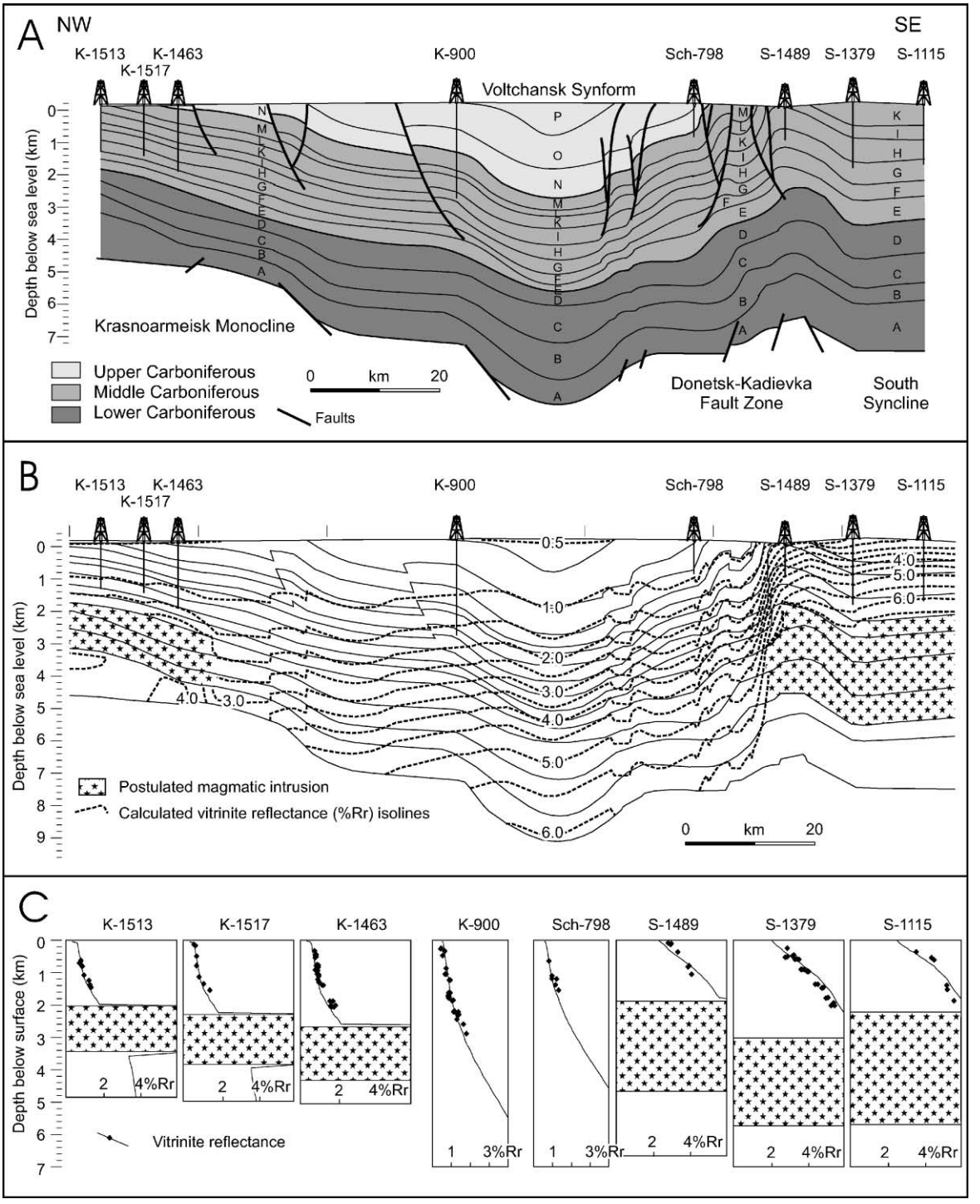
A
NW
SE
K-1513
K-1463
K-1517
K-900
Sch-798
S-1489
S-1379
S-1115
Voltchansk Synform
Depth below sea level (km)
Krasnoarmeisk Monocline
Upper Carboniferous
Middle Carboniferous
Lower Carboniferous
0 km 20
Faults
Donetsk-Kadievka Fault Zone
South Syncline
B
Postulated magmatic intrusion
Calculated vitrinite reflectance (%Rr) isolines
C
Depth below surface (km)
Vitrinite reflectance
2 4%Rr
1 3%Rr

Table 3
Properties assigned to liquid magma

Age [m.y.]	Intrusion temperature [°C]	Magma density [kg/m^3]	Solidus temperature [°C]	Magma thermal conductivity [W/m K]	Magma heat capacity [cal/g K]	Crystallisation heat [MJ/m]
270/265[a]	1000/900	1000	900/850	2.00	0.70	700

[a] First value: eastern intrusion, second value: western intrusion.

with calibration data. The intrusion model is based on Delaney (1988) and uses the values for liquid magma shown in Table 3. Convective heat transport was not considered.

4.2.2. Thermal history

Heat flow histories reconstructed with the 1-D approach were used as ''background heat flow'' in the 2-D model. The resulting thermal field is overprinted by the thermal effect of the modelled magmatic intrusions. Depth, shape, age, and temperature of the intrusions influence the thermal structure and the resulting vitrinite reflectance patterns. A satisfactory fit between measured and calculated calibration data (Fig. 11C) is obtained with a model including two shallow intrusions (see Fig. 11B for their present-day position). Fig. 12 represents calculated isotherms and the calculated vitrinite reflectance pattern for a 10-million-year-long time-interval during the Permian.

A westward decrease in heat flow during maximum burial (274 m.y.) resulted in a gentle dip of both isotherms and iso-reflectivity lines. Four million years after maximum burial, a shallow pluton intruded the western transect (South Syncline) at a depth of 5–6 km. A temperature of 1000 °C was adopted for this intrusion. Maximum heating and coalification of overlying rocks occurred within a very short timespan (0.2 m.y.). Thereafter, no change of vitrinite reflectance occurred along the eastern part of the transect. Then 265 m.y. before present, a pluton intruded the western profile (Krasnoarmeisk region) in an even shallower position (3–4 km depth) and with a slightly lower temperature (900 °C). The thermal effect matured middle Carboniferous rocks in the western part of the transect and vanished after a few hundred thousand years.

5. Discussion

The heat flow distribution during maximum burial is indicated by (hand-contoured) isolines in Fig. 10A. Although the isolines are rather speculative in some areas, they show some major trends. Heat flow during maximum burial was in the range of 40–75 mW/m^2. The Donbas Foldbelt (inverted part of the Donets Basin) was characterized by higher heat flow than the Krasnoarmeisk Monocline and the Kalmius–Torets Depression. In the latter areas, heat flow increased in a northeastward direction from 40 to 55 mW/m^2. East of Donetsk, heat flow was in the range of 60–75 mW/m^2 and increased towards the southeast. Both amplitude and distribution of paleo-heat flow, are similar to the present-day one (Gordienko et al., 1999). Unfortunately, paleo-heat flow east of the study area (central and eastern Donets Basin) cannot be reconstructed because of advanced coalification (>6% R_r) and the limitations of our approach (see Section 3.2).

Apart from a major increase in thickness of Permo-Carboniferous rocks towards the basin center (Fig. 10B), the lateral variations in Permian heat flow also contributed to the observed eastward increase in coalification of specific seams.

Permian erosion was 2–3 km in the Krasnoarmeisk and Kalmius–Torets regions. Erosion was significantly higher (>4 km) in the South and North Synclines east of the Donetsk–Kadievka fault (Fig. 10B). Interesting to note that the jump in Permian erosion follows the Donetsk–Kadievka Fault and roughly parallels the 60 mW/m^2 isoline of Permian heat flow (Fig. 10A).

Additional heating events are suggested for the South Syncline and northern Krasnoarmeisk regions.

Fig. 11. (A) NW–SE-trending transect through the western Donets Basin and position of calibration wells. See Figs. 4 and 10 for the location of cross section. (B) Computer-generated finite element model used for 2-D modelling. The position of postulated magmatic intrusions and the calculated vitrinite reflectance isolines are shown. (C) Calculated and measured vitrinite reflectance values for the calibration wells.

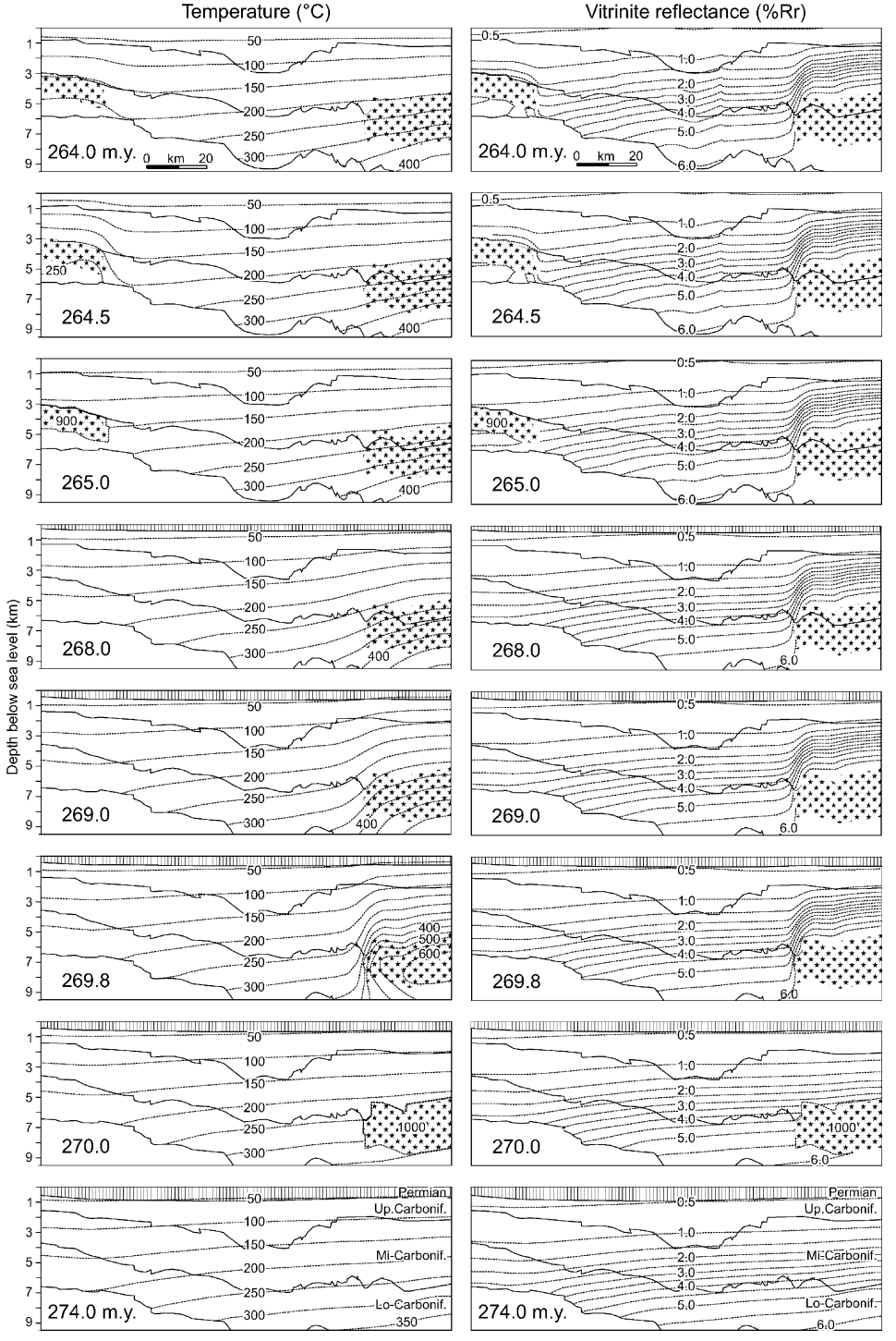
Temperature (°C)
Vitrinite reflectance (%Rr)
Depth below sea level (km)
264.0 m.y.
264.5
265.0
268.0
269.0
269.8
270.0
274.0 m.y.
0 km 20
Permian
Up.Carbonif.
Mi-Carbonif.
Lo-Carbonif.

The heating event in the South Syncline area can be interpreted by magmatic activity, which is postulated by Aleksandrov et al. (1996). They favour a late Permian age, which fits well with the applied 1-D and 2-D models. However, a final decision on age will be possible only after radiometric age dating (e.g. fission track analyses).

The heat source for the northern Krasnoarmeisk area is more speculative, since no indications for magmatism are known from this part of the basin so far. Heating by a late Permian magmatic body, which is slightly younger than the intrusion in the South Syncline, therefore remains speculative. In any case, it is remarkable that the studied wells are located at the northern tip of a SW–NE-trending zone with elevated vitrinite reflectance (see Fig. 3). We speculate that the latter may be a result of the same heating event. Further investigations will show whether coalification was due to increased basement heat flow or due to magmatic activity. Privalov (1998, 2000) distinguished several tectonic sectors within the Donets Basin. The Krasnoarmeisk area lies in sector C1, which according to his model was under extension during the late Permian. Perhaps local extension was related to the observed thermal event.

Reconstructed paleo-heat flows southwest of Donetsk are rather low. Low heat flows during maximum burial and the lack of evidence for a high heat flow event are remarkable, because they occur near an area where Permian magmatic stocks and sills metamorphosed Carboniferous coal (Jernovaya, 1997; Figs. 3 and 10). According to Privalov et al. (1998), these Permian sills and stocks (gabbro–monzonite–syenite complex) are slightly older than the magmatic bodies [(trachy–)andesite complex] in the South Syncline region and intruded during a compressional phase. Probably, the volume of the magma was not high enough to influence regional heat flow. Therefore, the hot magma only resulted in contact metamorphism.

The reconstructed thermal event, which occurred after maximum burial during the late Permian(?) in the South Syncline region, has consequences for our understanding of the evolution of the Donets Basin. The following aspects should be mentioned. A more thorough discussion is beyond the scope of the present paper.

- The thermal event helps explain the spatial distribution of epigenetic minerals in the basin (see Aleksandrov et al., 1996 and Fig. 4).
- Our results suggest that coal bed methane was generated not only during maximum burial, but also afterwards. Obviously, the late generated gas has a higher preservation potential. Therefore, the gas potential of the Donets Basin should be re-evaluated in the light of the new findings.
- The thermal effect of the magmatic event may have weakened the crust during Permian uplift.
- Unfortunately, the reconstructed thermal history does not help to ascertain whether main inversion occurred during the Permian or Cretaceous. The postulated syn-deformational, late Permian age agrees with both tectonic scenarios.

6. Conclusions

The applied numeric models suggest that different factors control coalification patterns in the western Donets Basin. Among these are:

- depth of Carboniferous rocks during maximum (Permian) burial,
- Permian uplift,
- lateral heat flow variations during maximum burial.

The resulting coalification pattern was overprinted by:

- Permian sills and stocks, which coked seams SW of Donetsk. The amount of heat transported by the magmatic rocks was not high enough to cause a regional heat flow anomaly.
- A heating event in the northern Krasnoarmeisk and the South Syncline regions. At least the latter is most probably caused by magmatic intrusions. Based

Fig. 12. Calculated temperature and vitrinite reflectance distributions for different Permian times (ages are shown in the lower left part of each plot). The thermal model considers heat flows, which were reconstructed by 1-D models for each well. The resulting temperature distribution is overprinted by magmatic intrusions.

on our models, we suggest a late Permian heating. However, Mesozoic ages cannot be excluded.

Acknowledgements

The investigations were undertaken as part of INTAS project 97-0743 and in the framework of the GeoRift project of Europrobe, a program of the European Science Foundation. The financial support of INTAS is gratefully acknowledged. Travel expenses of R.F.S. were partly covered by the Austrian Science Foundation (A-198-Tec). S.Sh. acknowledges support in the frame of an Ernst Mach Grant of the Austrian Academic Exchange Service. The paper benefited greatly from critical reviews by R. Schegg and J. Close.

References

Aleksandrov, A.L., Gordienko, V.V., Derevskaya, K.I., Zemskov, G.A., Ivanov, A.P., Panov, B.S., Shumlyanskiy, V.A., Epov, O.G., 1996. Deep Structure, Evolution of Fluid Systems and Endogenic Gold-Bearing Potentiality, South-Eastern Part of Ukrainian Donets Basin (in Russian). Institute of Fundamental Researches of Ukrainian Scientific Association, Kyiv, 74 pp.

Belokon, V.G., 1971. Geological history of evolution of the Donbas (in Russian). Geology and Prospecting of Coal Deposits. Nedra, Moscow, pp. 3–15.

Bostick, N.H., Foster, J.M., 1975. Comparison of vitrinite reflectance in coal seams and in kerogens of sandstones, shales and limestones in the same part of a sedimentary section. In: Alpern, B. (Ed.), Petrographie Organique et Potential Petrolier. CNRS, Paris, pp. 14–25.

Büker, C., 1996. Absenkungs-, Erosions- und Wärmeflußgeschichte des Ruhr-Beckens und des nördlichen Rechtsrheinischen Schiefergebirges. Berichte Forschungszentrum Jülich, Jülich, 250 pp.

Chekunov, A.V., Kaluzhnaya, L.T., Ryabchun, L.I., 1993. The Dniepr–Donets paleorift, Ukraine, deep structures and hydrocarbon accumulations. J. Pet. Geol. 16, 183–196.

de Boorder, H., van Beek, A.J.J., Dijkstra, A.H., Galetsky, L.S., Koldewe, G., Panov, B.S., 1996. Crustal architecture of the Donets Basin: tectonic implications for diamond and mercury–antimony mineralization. Tectonophysics 268, 293–309.

Delaney, P.T., 1988. Fortran 77 programs for conductive cooling of dikes with temperature-dependent thermal properties and heat of crystallisation. Comput. Geosci. 14, 181–212.

DOBREflection Working Group, 2000. The inverted Donbas Basin (Ukraine)—First results from DOBREflection in 2000. EUG XI. J. Conf. Abstr. 6 (1), p. 337.

DOBREfraction Working Group, 2001. DOBREfraction '99—velocity model of the crust and upper mantle beneath the Donbas Foldbelt (SE Ukraine). EGS, Abstract volume, Nice, p. 694.

Einor, O.L., 1996. The former USSR. In: Wagner, R.H. (Ed.), The Carboniferous of the world III, The former USSR, Mongolia, Middle Eastern Platform, Afghanistan, and Iran, IUGS Publ. 33. Instituto Geologico y Minero de Espana, Madrid, pp. 13–407.

Everlien, G., 1996. High-temperature programmed pyrolysis of Paleozoic source rocks from Northern Germany and adjacent areas and its thermodynamic constraints. Org. Geochem. 24, 985–998.

Gordienko, V.V., Zavgorodnyaya, O.V., Usenko, O.V., 1999. The heat flow of the Donets Basin. Geophys. J. 19, 209–214.

Grieve, R.A., 1982. The record of impact on Earth: implications for a major Cretaceous/Tertiary impact event. Geol. Soc. Am., Spec. Pap. 190, 25–37.

Harland, W.B., 1990. A Geologic Time Scale 1989. Cambridge Univ. Press, Cambridge, 263 pp.

Hertle, M., Littke, R., 2000. Coalification pattern and thermal modelling of the Permo-Carboniferous Saar Basin (SW-Germany). Int. J. Coal Geol. 42, 273–296.

Izart, A., Briand, C., Vaslet, D., Vachard, D., Coquel, R., Maslo, A., 1996. Stratigraphy and sequence stratigraphy of the Moscovian in the Donets basin. Tectonophysics 268, 189–209.

Jernovaya, G., 1997. Thermally metamorphosed coals from the southern Donbas, Ukraine. Proceedings of the XIII Int. Congress on the Carboniferous and Permian. Polish Geological Institute, Warsaw, pp. 75–78.

Lazarenko, E.K., Panov, B.S., Gruba, V.I., 1975. The Mineralogy of the Donets Basin, 1 (in Russian). Naukova dumka, Kiev, 225 pp.

Levenshtein, M.L., Lagutina, V.V., Kaminsky, V.V., 1991a. Explanations to the Maps of Thicknesses and Structure of Middle Carboniferous Coal Seams in the Donetsk Coal Basin (in Russian). Ministry of Geology of the USSR, Kiev, 100 pp.

Levenshtein, M.L., Spirina, O.I., Nosova, K.B., Dedov, V.S., 1991b. Map of Coal Metamorphism in the Donetsk Basin (Paleozoic surface). 1:500 000. Ministry of Geology of the USSR, Kiev.

Maidanovitch, I.A., Radzivill, A.Ya., 1984. The Peculiarities of Tectonics of Coal Basins of Ukraine (in Russian). Naukova dumka, Kiev, 120 pp.

Makarov, I.A., 1982. Description of the stratigraphic cross-sections of the lower and middle Carboniferous of the Donets basin (in Russian). Ukr. Geol. Minist., PGO Donbas Geology, Artemovsk GPE.

Makarov, I.A., 1985. Description of the stratigraphic cross-sections of the upper Carboniferous of the Donets basin (in Russian). Ukr. Geol. Minist., PGO Donbas Geology, Artemovsk GPE.

Marshall, J.S., Pilcher, R.C., Bibler, C.J., 1996. Opportunities for the development and utilization of coal bed methane in three coal basins in Russia and Ukraine. In: Gayer, R., Harris, I. (Eds.), Coalbed Methane and Coal Geology. Geol. Soc., Spec. Publ., vol. 109. The Geological Society, Bath, pp. 89–101.

Minesterstvo Geologii SSSR, 1983. Geological map of the USSR and adjoining water-covered areas. Scale 1:2 500 000. 1983. Minesterstvo Geologii SSSR, BSEGEI.

Movshovich, E.V., Milyavsky, A.E., 1985. On age of Kamensky astrobleme and some peculiarities of its structure (in Russian). Geol. J. 3, 67–75.

Nagorny, Yu.N., Nagorny, V.N., 1976. Peculiarities of geological evolution of the Donets Basin (in Russian). Geotectonica 1, 74–86.

Nesterenko, L.P., 1978. Early Permian Deposits of the Kalmius–

Torets Depression in the Donets Basin (in Russian). Vischa shkola, Kiev, 148 pp.

Nikolskiy, J.L., Buturlinov, N.V., Panov, B.S., Korcemagin, V.A., 1973. Beitrag zur Metallogenese des Donezbeckens (UdSSR). Z. Angew. Geol. 19, 505–508.

Panov, B.S., 1999. On pollution of the biosphere in industrial areas: the example of the Donets coal Basin. Int. J. Coal Geol. 40, 199–210.

Privalov, V.A., 1998. Block rotations and scenario of the tectonic evolution of the Donets Basin (in Russian). Geol. Geochem. Fossil Fuel Deposits 4, 142–158.

Privalov, V.A., 2000. Local extension as factor governing the localisation of centres of magmatism and endogenous mineralization in the Donbas (in Russian). Trans. Donetsk State Tech. Univ. 11, 115–120.

Privalov, V.A., Panova, E.A., Azarov, N.Ya., 1998. Tectonic events in the Donets Basin: spatial, temporal and dynamic aspects (in Russian). Geol. Geochem. Fossil Fuel Deposits 4, 11–18.

Starostenko, V.I., Danilenko, V.A., Vengrovitch, D.B., Kutas, R.I., Stovba, S.M., Stephenson, R.A., Kharitonov, O.M., 1999. A new geodynamical–thermal model of rift evolution, with application to the Dnieper–Donets Basin, Ukraine. Tectonophysics 313, 29–40.

Stephenson, R.A., Stovba, S.M., Starostenko, V.I., 2001. Pripyat–Dniepr–Donets Basin: implications for dynamics of rifting and the tectonic history of the northern Peri-Tethyan platform. In: Ziegler, P.A., et al. (Eds.), Peri-Tethyan Rift/Wrench Basins and Passive Margins, Peri-Tethys Memoir 6, vol. 186. Mémoires du Muséum National d'Histoire Naturelle, Paris, pp. 369–406.

Sterlin, B.P., Makridin, V.P., Lutsky, P.I., 1963. Stratigraphy of Mesozoic and Cenozoic deposits of the Donets Basin (in Russian). Geology of Coal and Oil Shale Deposits of the USSR 1. Nedra, Moscow, pp. 64–88.

Stovba, S.M., Stephenson, R.A., 1999. The Donbas Foldbelt: its relationships with the uninverted Donets segment of the Dniepr–Donets Basin, Ukraine. Tectonophysics 313, 59–83.

Sweeney, J.J., Burnham, A.K., 1990. Evaluation of a simple model of vitrinite reflectance based on chemical kinetics. Am. Assoc. Pet. Geol. Bull. 74, 1559–1570.

Taylor, G.H., Teichmüller, M., Davis, A., Diessel, C.F.K., Littke, R., Robert, P., 1998. Organic Petrology. Borntraeger Berlin, Stuttgart, 704 pp.

van Wees, J.D., Stephenson, R.A., Stovba, S.M., Shymanovskyi, V.A., 1996. Tectonic variation in the Dniepr–Donets Basin from automated modelling of backstripped subsidence curves. Tectonophysics 268, 257–280.

Walker, S., 2000. Major coalfields of the world. IEA Coal Res. CCC/32, 131 pp.

Welte, D.H., Horsfield, B., Baker, D.R., 1997. Petroleum and Basin Evolution. Springer, Berlin, 535 pp.

Yalcin, M.N., Littke, R., Sachsenhofer, R.F., 1997. Thermal history of sedimentary basins. In: Welte, D.H., et al. (Eds.), Petroleum and Basin Evolution. Springer, Berlin, pp. 73–167.

Zhykalyak, M.V., Privalov, V.A., Ilnitsky, L.I., Panova, E.A., 2000. Relationships between Hercynian, Cimmerian and Alpine deformation patterns in the Donbas Foldbelt. Geophys. J. (Kyiv) 22, 143–144.